

PROCEEDINGS OF THE XIII FEOFILOV SYMPOSIUM
“SPECTROSCOPY OF CRYSTALS DOPED
BY RARE-EARTH AND TRANSITION-METAL IONS”

(Irkutsk, July 9–13, 2007)

A Phototropic Center and Distribution of the Chromium
Impurity in Rare-Earth Garnet Crystals

S. S. Kolesnikov and L. I. Shchepina

Institute of Applied Physics, Irkutsk State University, bulv. Gagarina 20, Irkutsk, 664033 Russia

e-mail: schepina@ari.isu.ru

Abstract—Crystals of two types, namely, $\text{Gd}_3\text{Sc}_2\text{Al}_3\text{O}_{12}$ doped by Ca^{2+} and Cr^{3+} ions and $\text{Gd}_3\text{Sc}_2\text{Ga}_3\text{O}_{12}$ doped by Nd^{3+} and Cr^{3+} , are studied using x-ray diffraction. In order to elucidate how an impurity is embedded in the lattice, its effect on the electron density distribution and microstrains of the crystal lattice is investigated. It is shown that chromium ions can occupy the lattice sites located predominantly in the octahedral environment of the oxygen ligands.

PACS numbers: 61.72.Dd, 61.72.Ff

DOI: 10.1134/S1063783408090254

1. INTRODUCTION

Interest in phototropic centers in garnets can be traced to the fact that their absorption falls into the region of lasing transitions of the Nd^{3+} ion (one of the most widely used laser ions). These crystals were employed to realize passive mode locking and passive Q switching of the neodymium laser and to demonstrate the possibility of development of high-efficiency lasers tunable over the wavelength range 1.4–1.6 μm [1, 2]. The majority of researchers [3–5] believe that phototropic centers are quadrivalent chromium ions which substitute in garnet-based crystals for Al^{3+} and Ga^{3+} ions and reside in the tetrahedral environment of oxygen ligands. These centers (Cr^{4+})_{tetr} are responsible for absorption of the crystal with a maximum at 1.06 μm and luminescence in the range 1.52–1.56 μm [6]. Il'ichev et al. [7] proposed an alternative model for the phototropic center based on the (Cr^{3+})_{oct} chromium ion. Our earlier experimental studies performed by optical spectroscopy yielded the following results [8]:

(1) Amplification of the luminescence (0.73 μm) of the Cr^{3+} ion by the second neodymium-laser harmonic, with the 1.54- μm luminescence intensity (due to the Cr^{4+} ion) remaining unchanged in the gadolinium–scandium–aluminum garnet doped by Ca and Cr (GSAG–Ca,Cr), as contrasted with the decrease in Cr^{3+} photoluminescence in the gadolinium–scandium–gal-

lium garnet doped by Cr and Nd (GSGG–Cr,Nd). These observations cast doubt on the validity of the interpretation of the absorption bands in the range 0.775–1.26 μm and the luminescence at 1.103–1.67 μm as originating from electronic transitions in Cr^{4+} ions occupying tetrahedral sites of the rare-earth garnet.

(2) The radiating oscillator is directed along the fourfold axis (C_4). Crystals of cubic symmetry in which the garnets under study crystallize are known to have three fourfold axes directed parallel to the cube edges. Along these directions can lie three groups of linear oscillators describing the radiation at $\lambda_m = 1.54 \mu\text{m}$. The chromium ion in the octahedral environment possesses this property to a larger extent than the tetrahedrally coordinated Cr^{4+} . The present study was aimed at collecting additional information on the chromium coordinates in the rare-earth garnet lattice by x-ray diffraction.

2. OBJECTS OF THE INVESTIGATION

The experiments were performed with rare-earth garnet crystals of two types, more specifically, GSAG doped by Ca^{2+} and Cr^{3+} and GSGG doped by Nd^{3+} and Cr^{3+} . The impurities uncontrollable during crystal growth and contained in the crystals were identified by the emission spectrum analysis. The results obtained are presented in the table.

Impurity content (in wt %) in garnet crystals according to the results of the emission spectrum analysis

Crystal	Mg	Ca	Cu	Ti	Si	Cr
$\text{Gd}_3\text{Sc}_2\text{Al}_3\text{O}_{12} : \text{Ca,Cr}$	$<3 \times 10^{-4}$	1.0	$2 \times 10^{-4} - 6 \times 10^{-4}$	–	$<10^{-3}$	1.5
$\text{Gd}_3\text{Sc}_2\text{Ga}_3\text{O}_{12} : \text{Cr,Nd}$	$<10^{-3}$	–	$10^{-4} - 3 \times 10^{-4}$	$<10^{-3}$	$\approx 10^{-3}$	0.5

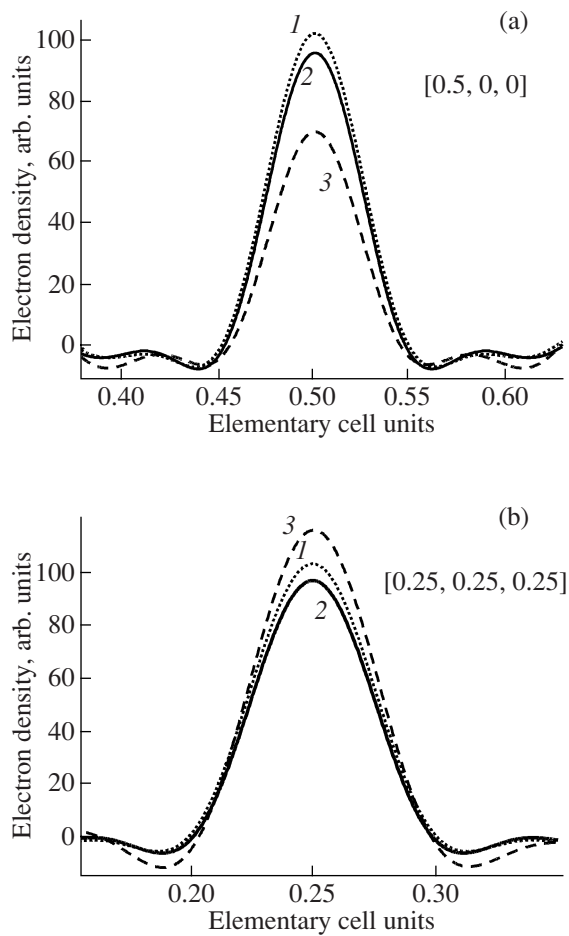


Fig. 1. Electron density distribution in scandium sites along the (a) $[0.5, 0, 0]$ and (b) $[0.25, 0.25, 0.25]$ directions in the GSAG crystals: (1) calculation for the model x-ray diffraction pattern (lattice without impurities) and (2, 3) the same for the experimental x-ray diffraction patterns with and without regard for the superstructure lines, respectively.

3. EXPERIMENT

The samples were studied using the x-ray powder diffraction analysis. The x-ray powder diffraction patterns were recorded on a DRON-3M diffractometer with a GUR-8 goniometer focused according to the Bragg–Brentano technique. The measurements were performed in the angular range from 15° to 135° . We determined the lattice parameters, estimated the microstrains, and calculated the electron densities at the lattice sites from the dependence of the scattering intensity on the diffraction angle.

4. RESULTS OF THE MEASUREMENTS AND DISCUSSION

The electron densities were calculated by summation of the Fourier expansions

$$\rho(x, y, z) = \frac{1}{V} \sum_{hkl=-15}^{15} \sum \sum F(hkl) \times \cos \left[\frac{2\pi}{a} (hx + ky + lz) \right],$$

where $F(hkl)$ are structure amplitudes extracted from the diffraction reflection intensities. The signs of the amplitudes were found from model considerations and the known garnet structure [9]. Indexing the diffraction patterns obtained for the GSAG crystals revealed the existence of peaks forbidden for the given symmetry. The garnet structure being bcc, one should expect that the extinction rules for the given symmetry are satisfied. In other words, an x-ray diffraction pattern should contain only the reflections with an even sum of the hkl indices. For the GSGG sample this rule is fully met. By contrast, the diffraction patterns of the GSAG samples exhibit several peaks for which it is not met; more specifically, while their hkl indices are determined as they should be for a cubic lattice with the same parameter as the main lattice, the hkl values themselves are forbidden for the given symmetry. This can be assigned to the existence of a superstructure in the sample under study, i.e., the impurity enters the main lattice in an ordered manner [10].

The experimental data were used to calculate the two-dimensional sections of electron densities for the coordinates $z = 0, 0.125, 0.25, 0.375,$ and 0.5 . Out of these two-dimensional sections we selected such one-dimensional sections which contained electron densities of the ions of interest.

We performed the above procedure for the electron density calculated with and without allowance for the superstructure lines, as well as for a model x-ray diffraction pattern constructed with the PowderCell code for an impurity-free lattice. The results are shown in Figs. 1–4. An analysis of Fig. 1a suggests that the electron density at the scandium sites in the GSAG crystal is substantially lower than that calculated for the model diffraction pattern. This can mean that the impurity entering on the $(x, 0, 0)$ sites has a smaller atomic number; calcium is such an impurity. On the other hand, a reverse pattern is seen in Fig. 1b. An impurity with a larger atomic number, namely, chromium enters on the site with the coordinates $(0.25, 0.25, 0.25)$ in the GSAG crystal. No substantial discrepancies of the calculated values derived from experiment are seen from the values obtained for the model diffraction pattern in any electron density distribution for the Gd and Al ions (Fig. 2), which practically excludes the possibility for an impurity to enter on these sites. It can be suggested that the Ca and Cr dopants enter the lattice by forming a superstructure, because the electron densities which were constructed from data obtained without allowing for the superstructure lines do not practically differ (within experimental accuracy) from those obtained for the model lattice.

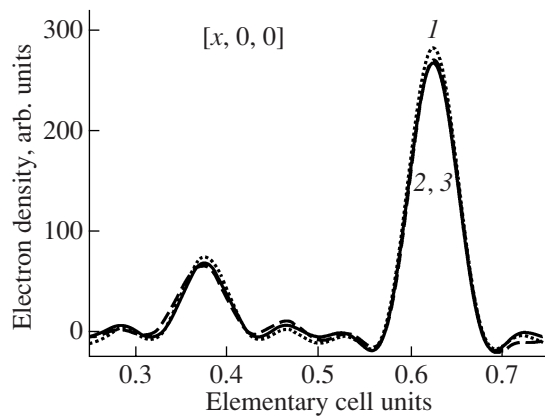


Fig. 2. Electron density distribution in the Al and Gd sites in the structure of the GSAG crystals: (1) calculation for the model x-ray diffraction pattern (lattice without impurities) and (2, 3) the same for the experimental x-ray diffraction patterns with and without regard for the superstructure lines, respectively.

Thus, the scenario obtained for the garnet of this type (GSAG) is as follows: Ca substitutes for Sc at the coordinates (0, 0, 0) and (0.5, 0, 0) and Cr substitutes for Sc at the coordinates (0.25, 0.25, 0.25). In other words, the impurity ions are incorporated into the lattice in an ordered way to form a superstructure apparently because the divalent Ca ion substitutes for the trivalent Sc, with the Cr^{4+} ion entering on the nearest scandium site to balance the charge. The possibility for Cr^{4+} to become inserted into the tetrahedral sites occupied by Al^{3+} ions is practically excluded.

For the second type of crystals (GSGG), one-dimensional sections of electron densities were constructed along the same directions as in the preceding case. The results obtained are as follows (Figs. 3, 4). The electron density at the Sc sites calculated for the model x-ray diffraction pattern is substantially lower than that for the experimental one. This follows from the electron density distributions displayed in Figs. 3a and 3b; i.e., the impurity with a larger atomic number becomes inserted at the above coordinates in place of Sc. As already mentioned, the samples of the second type (GSGG) were doped by neodymium and chromium. Both these impurities having larger atomic numbers, it can be assumed that scandium is replaced either by both these impurities or by one of them only. We note the identical variations in the electron densities along different Sc coordinates (to be contrasted with the preceding case of GSAG). The impurity becomes incorporated in a disordered manner to form an equilibrium substitutional solid solution in these GSGG crystals. As for the electron density distributions at gallium and gadolinium sites, no pronounced differences between the model and experimental patterns are observed either for gallium or for gadolinium (Fig. 4).

The above results agree with the experimental data obtained by optical methods [8]. This applies, in partic-

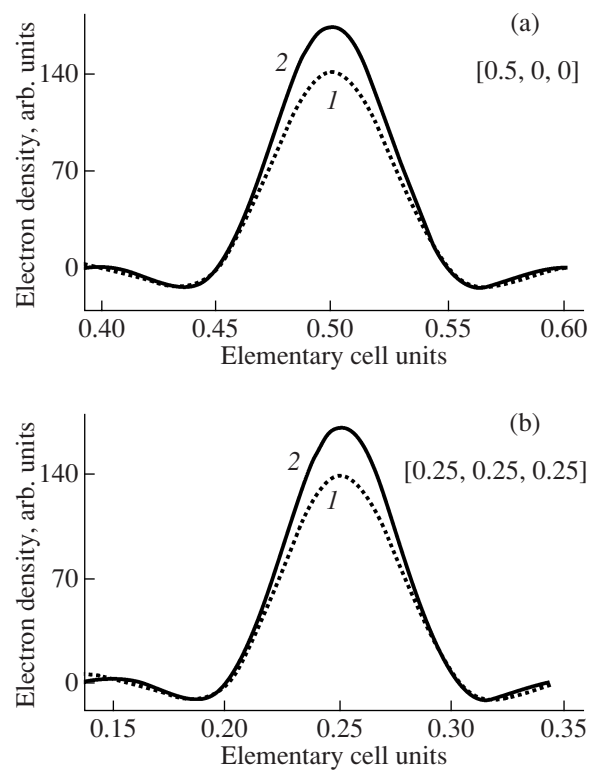


Fig. 3. Electron density distribution in the scandium sites along the (a) [0.5, 0, 0] and (b) [0.25, 0.25, 0.25] directions in the GSGG crystals: (1) calculation for the model x-ray diffraction pattern (lattice without impurities) and (2) experimental data.

ular, to photoconversion of defects by the second harmonic of the neodymium laser, where one observes enhancement of the Cr^{3+} luminescence in GSAG(Ca,Cr) and weakening of the Cr^{3+} luminescence in GSGG(Cr,Nd) crystals. One can envisage here the following reactions: $\text{Cr}^{4+} + e \rightarrow (\text{Cr}^{3+})^* \rightarrow h\nu + \text{Cr}^{3+}$; $\text{Cr}^{3+} + h\nu \rightarrow \text{Cr}^{4+}$, if Cr^{4+} and Ca^{2+} ions become incorporated into the rare-earth garnet lattice during crystal growth to form a superstructure. The above pro-

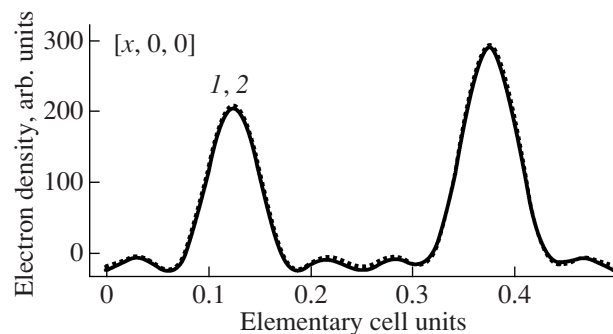


Fig. 4. Electron density distribution in the Ga and Gd sites along the [x, 0, 0] direction in the GSGG crystals: (1) calculation for the model x-ray diffraction pattern (lattice without impurities) and (2) experimental data.

cesses occurring simultaneously culminate in a balance in the concentration of Cr^{3+} ions. The equilibrium can be disrupted if the concentration of chromium ions with a valence of 4+ in the crystal is larger than that of the trivalent ions. In this case, one observes enhancement of the Cr^{3+} luminescence, as this occurs in the GSAG-(Ca,Cr) samples. And conversely, the Cr^{3+} luminescence intensity is lower if the concentration of the Cr^{3+} ions is higher by far than that of the photoinduced Cr^{4+} ions (the GSGG-(Cr,Nd) samples, where the Cr^{3+} ions are inserted to form an equilibrium substitutional solid solution).

5. CONCLUSIONS

Thus, impurity ions substitute for scandium ions in both samples; however, in GSAG, calcium and Cr^{4+} are embedded along different coordinates with the formation of a superstructure, whereas in GSGG, neodymium and Cr^{3+} are embedded in the lattice with an equal probability over all coordinates of scandium, thus forming an equilibrium substitutional solid solution. The probability for Cr^{4+} to be located in the tetrahedral sites occupied by Al^{3+} or Ga^{3+} is practically zero.

REFERENCES

1. Wang Su-Mei, Feng Bao-Hua, Zhang Qiu-Lin, Zhang Dong-Xiang, and Zhang Shi-Wen, *Chin. Phys. Lett.* **22**, 877 (2005).
2. V. B. Tsvetkov, G. A. Bufetova, D. A. Nikolaev, V. F. Seregin, I. A. Shcherbakov, M. Yu. Gusev, and I. A. Ivanov, *Laser Phys.* **15**, 579 (2005).
3. L. I. Krutova, N. A. Kulagin, V. A. Sandulenko, and A. V. Sandulenko, *Fiz. Tverd. Tela (Leningrad)* **31** (7), 170 (1989) [*Sov. Phys. Solid State* **31** (7), 1193 (1989)].
4. V. I. Garmash, V. A. Zhitnyuk, and A. G. Okhrimchuk, *Izv. Akad. Nauk SSSR, Neorg. Mater.* **26**, 1700 (1990).
5. L. G. Popov, Extended Abstracts of Candidate's Dissertation (Irkutsk State University, Irkutsk, Russia, 1994) [in Russian].
6. J. A. Caird, E. F. Krupke, M. D. Shinn, in *Technical Digest of Conference on Lasers and Electro-Optics* (Optical Society of America, Baltimore, MD, United States, 1985), p. 232.
7. N. N. Il'ichev, A. V. Kir'yanov, P. P. Pashinin, and S. Kh. Shpuga, *Zh. Éksp. Teor. Fiz.* **105** (5), 1426 (1994) [*JETP* **78** (5), 768 (1994)].
8. L. I. Shchepina, O. V. Borodina, and L. I. Ruzhnikov, *Pis'ma Zh. Tekh. Fiz.* **31** (6), 23 (2005) [*Tech. Phys. Lett.* **31** (3), 228 (2005)].
9. C. A. Geiger and T. Armbruster, *Am. Mineral.* **82**, 740 (1997).
10. Ya. S. Umanskiĭ, *X-Ray Diffraction Analysis of Metals and Semiconductors* (Metallurgiya, Moscow, 1969) [in Russian].

Translated by G. Skrebtsov